

DENSYS

MASTER ERASMUS MUNDUS DECENTRALISED SMART ENERGY SYSTEMS



UNIVERSITAT POLITÈCNICA
DE CATALUNYA
BARCELONATECH

Delivery of Assignment

for

Turbulence

Submitted to

Prof. Xavier Trias

January 2, 2024

Seyed Mohammadamin Taleghani

Table of Contents

1. Problem Specification.....	5
2. Average Flow Features	5
2.1. Average Velocities.....	5
2.2. Average Reynolds Stresses	7
3. Kolmogorov Length Scale	9
4. Kinetic Energy and Turbulent Kinetic Energy	11
5. Lift and Drag Dynamics	12
6. Conclusion	13
7. References	13
8. Appendix I: MATLAB Code	14

Table of Figures

Figure 1. Schematic of the square cylinder problem. Above: side view of the domain. Below: top view of the domain. [1].....	5
Figure 2. Average horizontal velocity profiles at different stream-wise locations. Left: the profiles for the whole domain height. Right: zoomed view of the profiles near the obstacle. ..	6
Figure 3. Normal Reynolds Stresses at $x = 0.0$ in: stream-wise direction (left), cross-stream direction (right), span-wise direction (bottom).....	8
Figure 4. Reynolds Shear Stress at $x = 0.0$	8
Figure 5. Normal Reynolds Stresses at $x = 0.0$ compared to $x = 1.0$ in: stream-wise direction (left), cross-stream direction (right), span-wise direction (bottom).....	9
Figure 6. Reynolds Shear Stress at $x = 0.0$ compared to $x = 1.0$	9
Figure 7. The ratio of the stream-wise grid spacing and Kolmogorov length scale.	10
Figure 8. The ratio of the cross-stream grid spacing and Kolmogorov length scale.	11
Figure 9. The kinetic energy of the average velocity field. Left: overall view. Right: body region.	11
Figure 10. Turbulent kinetic energy of the average velocity field. Left: overall view. Right: body region.	12
Figure 11. Time variation of the Lift and Drag Coefficient.	13

Abbreviations

Boundary Layer

BL

Shear Layer

SL

Turbulent Kinetic Energy

TKE

Mean Kinetic Energy

MKE

1. Problem Specification

This problem analyzes the flow around a square cylinder at a Reynolds number of 22,000. The dimensionless Reynolds number (Re) depends on the incoming flow velocity (U) and the cylinder width (D). The computational domain is $30.5D$ long (streamwise), $54D$ wide (cross-stream), and πD deep (spanwise). The cylinder's front face is located $10D$ downstream from the inlet and is centered between the side boundaries. The coordinate origin is placed at the cylinder's center.

The inlet has a constant velocity profile of $u = (U, 0, 0)$, while the outlet uses convective boundary conditions. No-slip walls bound the cylinder surface. The side boundaries are periodic to allow for spanwise homogeneous turbulence, with a Neumann condition enabling cross-stream velocity gradients.

Results are made dimensionless, with D , U , D/U , and $\rho U^2/2$ as reference length, velocity, time, and pressure, respectively. A schematic of the problem is shown in Figure 1, and a fully commented version of the script used to analyze the simulation results is provided in Appendix I.

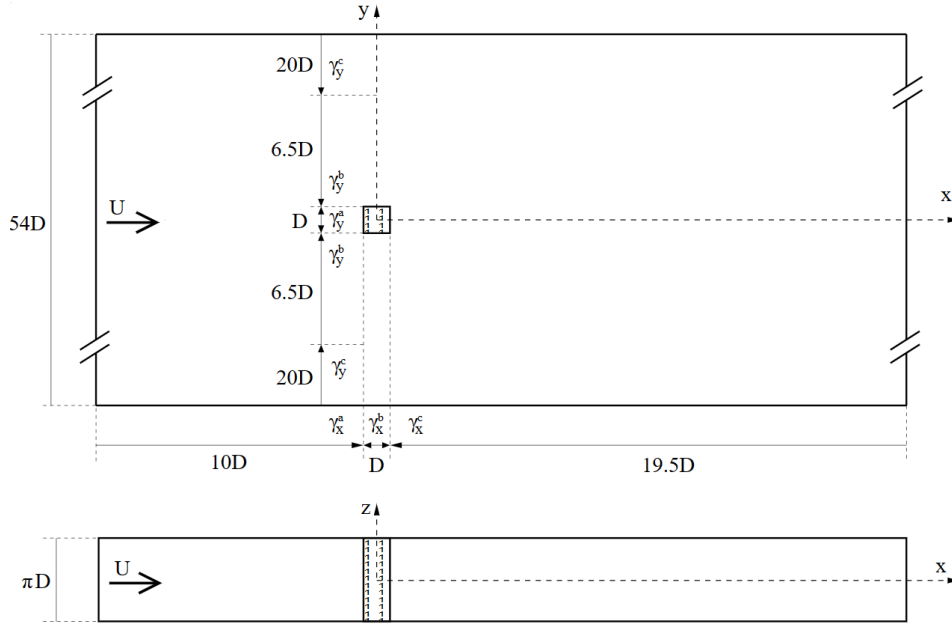


Figure 1. Schematic of the square cylinder problem. Above: side view of the domain. Below: top view of the domain. [1]

2. Average Flow Features

This section of the report examines averaged flow quantities to describe the key physics around a square obstacle.

2.1. Average Velocities

Figure 2 and Figure 9 display the average u and v components of the velocity vector at various x and y locations, respectively. In the left panel of Figure 2, a zoomed-out view of the velocity profiles reveals that as we transition from the top and bottom of the domain towards the obstacle, the velocity increases from 1.0 (the uniform inlet value) to over 1.4 at $x=0.0$ when

reaching the edge of the Boundary Layer (BL), then rapidly decreases upon entering the BL. This phenomenon is attributed to the obstacle and its thick BL, which restricts the area for the inviscid flow above it, leading to an increase in velocity in the inviscid region.

In the right panel of Figure 2, a zoomed-in view of the horizontal velocity profile is presented. The profile corresponding to $x = -0.5$ depicts the horizontal component of velocity at the location of the obstacle's upstream face. The red triangles on the profiles at the middle and end of the obstacle ($x = 0.0$ and $x = 0.5$) indicate the presence of reverse flow in the boundary layer of the top and bottom face, signifying separated BL in these regions. The red circles represent the approximate thickness of the BL. It is evident that the BL thickness for $x = 0.0$ is lower than that for $x = 0.5$. For the $x = 1.5$ curve, as the obstacle has ended by that point, a Shear Layer (SL) with lower momentum inside (low but not reversed) is observed, and its approximate edge is denoted by a red circle. Lastly, the profiles indicate a symmetry of the average values of velocity components.

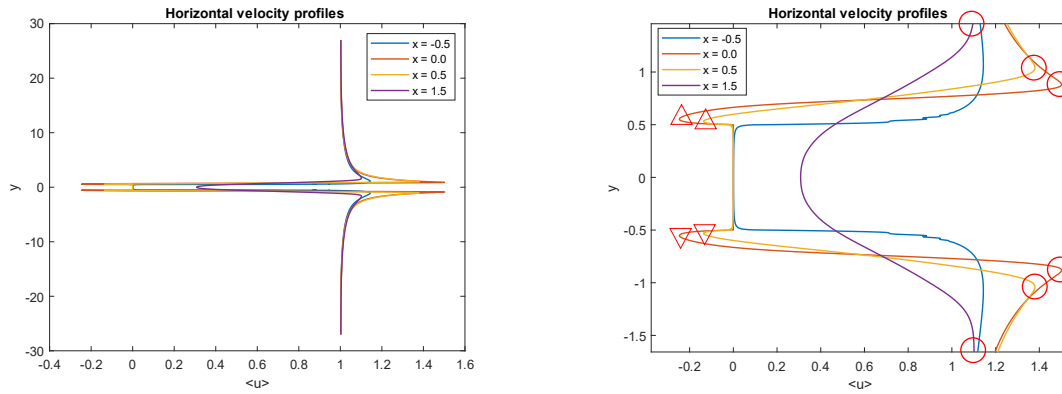


Figure 2. Average horizontal velocity profiles at different stream-wise locations. Left: the profiles for the whole domain height. Right: zoomed view of the profiles near the obstacle.

Figure 3 depicts the average vertical velocity profiles of the flow. In the zoomed-out view (left), it is evident that at the cross-stream heights of $y = -0.5$ and $y = 0.5$, there is a sharp peak in the vertical velocity due to the presence of the upstream face of the object, which induces an upward/downward flow along its surface. Subsequently, as the flow reaches the sharp corner of the square, the no-slip condition forces the vertical component to become zero.

In the zoomed-in view, it is observable that vertical velocities on the top half of the domain exhibit a positive peak, zero, and then a negative peak (indicated by red circles), while those in the bottom half of the domain undergo a negative peak, zero, and then a positive peak (indicated by red triangles). These patterns signify the presence of clockwise and anticlockwise rotating vortices on the top and bottom sides of the square, respectively. The center of this vortex is estimated to be located around the x -coordinate, where the vertical velocity becomes zero, approximately at $x = 0.35$. This observation aligns with the findings from the simulation video. Furthermore, it is noted that the $y = \pm 1.0$ curves exhibit a higher peak than $y = \pm 0.5$, indicating that those curves with a higher peak in vertical velocity are situated further away from the center of the vortex than the latter.

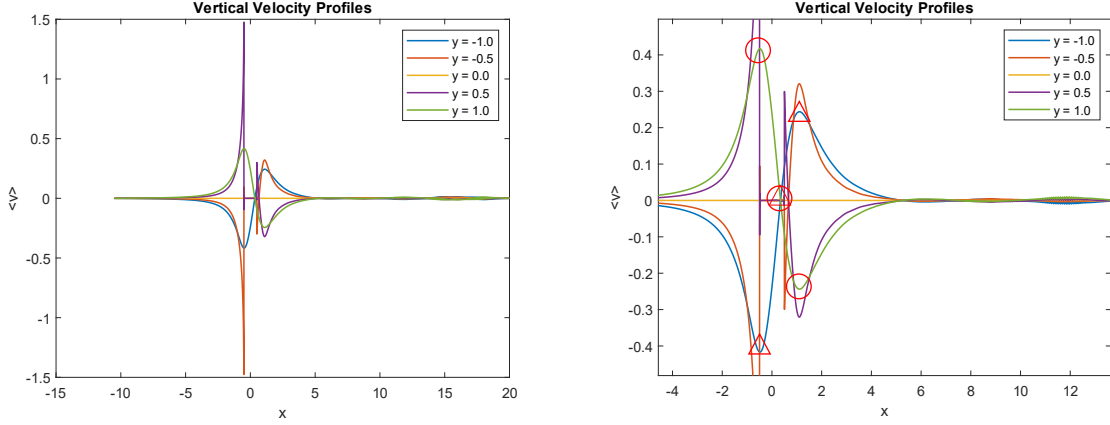


Figure 3. Average vertical velocity profiles at different cross-stream locations. Left: the profiles for the whole domain height. Right: zoomed view of the profiles near the obstacle.

2.2. Average Reynolds Stresses

In this section, we will delve into the analysis of the Reynolds stresses in the flow domain. Before we proceed, it's essential to provide some explanations regarding these quantities. We typically refer to $\rho \langle u'^2 \rangle$, $\rho \langle u'v' \rangle$, $\rho \langle u'w' \rangle$, and so on, as the Reynolds stresses, as their gradients have the dimensions of a force per unit volume. They are, however, only apparent stresses, as they arise from the non-linear convective terms in the Navier-Stokes equations [2]. Therefore, the normal Reynolds stress $\rho \langle u'^2 \rangle$ is actually an extra momentum flux of the face normal to the x direction, in addition to the momentum transfer by the mean flow. Similarly, $\rho \langle u'v' \rangle$ represents an extra mean shear stress on the face normal to y-direction. A similar term will arise when we consider the mean y-momentum passing through the face to be normal to x-direction so that the Reynolds stress tensor is symmetric.

Therefore, the normal Reynolds stress $\rho \langle u'^2 \rangle$ actually represents an additional momentum flux normal to the face in the x-direction, in addition to the momentum transfer by the mean flow. Similarly, $\rho \langle u'v' \rangle$ represents an additional mean shear stress on the face normal to the y-direction. A similar term arises when we consider the mean y-momentum passing through the face normal to the x-direction, resulting in the Reynolds stress tensor being symmetric.

With the above explanations, we can proceed to analyze the figures.

Figure 3 displays the normal Reynolds stresses in three directions: stream-wise (left), cross-stream (right), and span-wise (bottom) at $x = 0.0$. It is evident that the stream-wise normal Reynolds stress has the highest magnitude among the three directions. This is because the mean flow is in this direction; the cross-stream stress is the smallest due to the dampening of turbulent fluctuations by the upper and lower faces of the obstacle [3]. In all three figures, it is noticeable that the turbulent stresses are significant only inside the boundary layer (BL) and reduce to almost zero outside the BL.

In the stream-wise normal Reynolds stress, there is a momentary reduction at the height of $y = 0.6$. This is likely due to reverse flow in the BL slowing down the growth of turbulence in the x-direction. Overall, it appears that the growth of turbulence in the stream-wise direction is approximately six times larger than the growth of turbulence in the cross-stream and span-wise directions when we are at the middle of the obstacle.

Figure xxx compares the Reynolds stresses at $x = 0.0$ to $x = 1.0$. From the left figure, it is evident that the normal Reynolds stress in the x-direction is smaller due to the slower-moving mass of air in the wake region. The right figure shows a significant increase in cross-stream Reynolds stress. This is attributed to the removal of constraints that the obstacle was imposing on the turbulence growth in the vertical direction, leading to much faster growth of turbulence in the cross-stream direction. The turbulence in the spanwise direction has also grown, as evidenced by the bottom image. However, the magnitude of the turbulence in this direction has not changed significantly. The shear Reynolds stress has also increased significantly, indicating the heightened effect of turbulent shear stresses on the x-momentum, hence the designation “shear layer”.

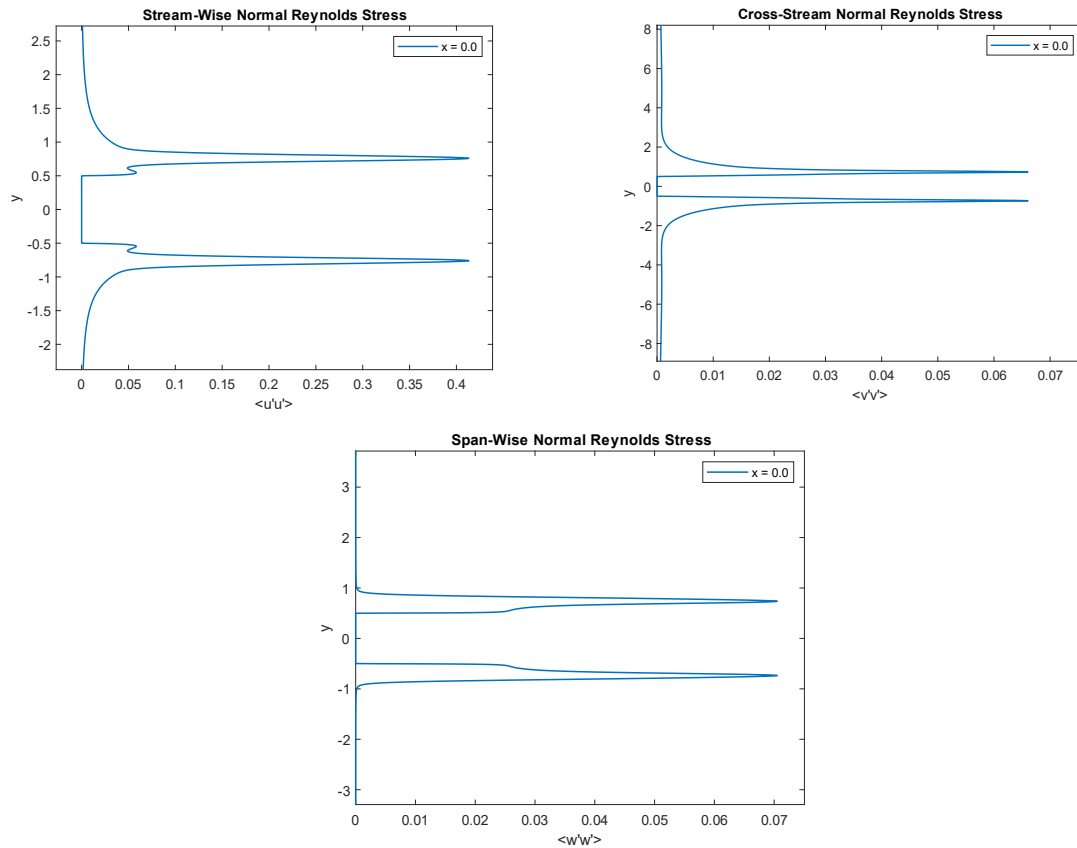


Figure 3. Normal Reynolds Stresses at $x = 0.0$ in: stream-wise direction (left), cross-stream direction (right), span-wise direction (bottom).

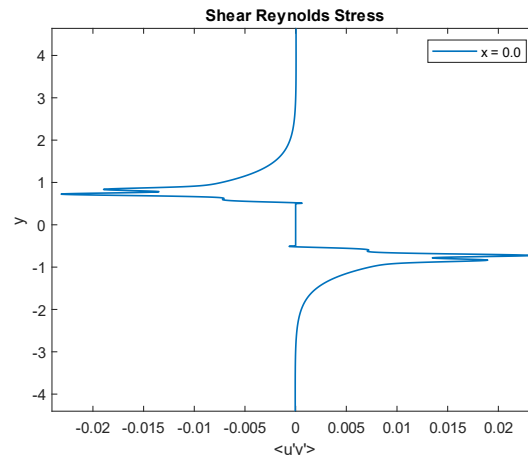


Figure 4. Reynolds Shear Stress at $x = 0.0$.

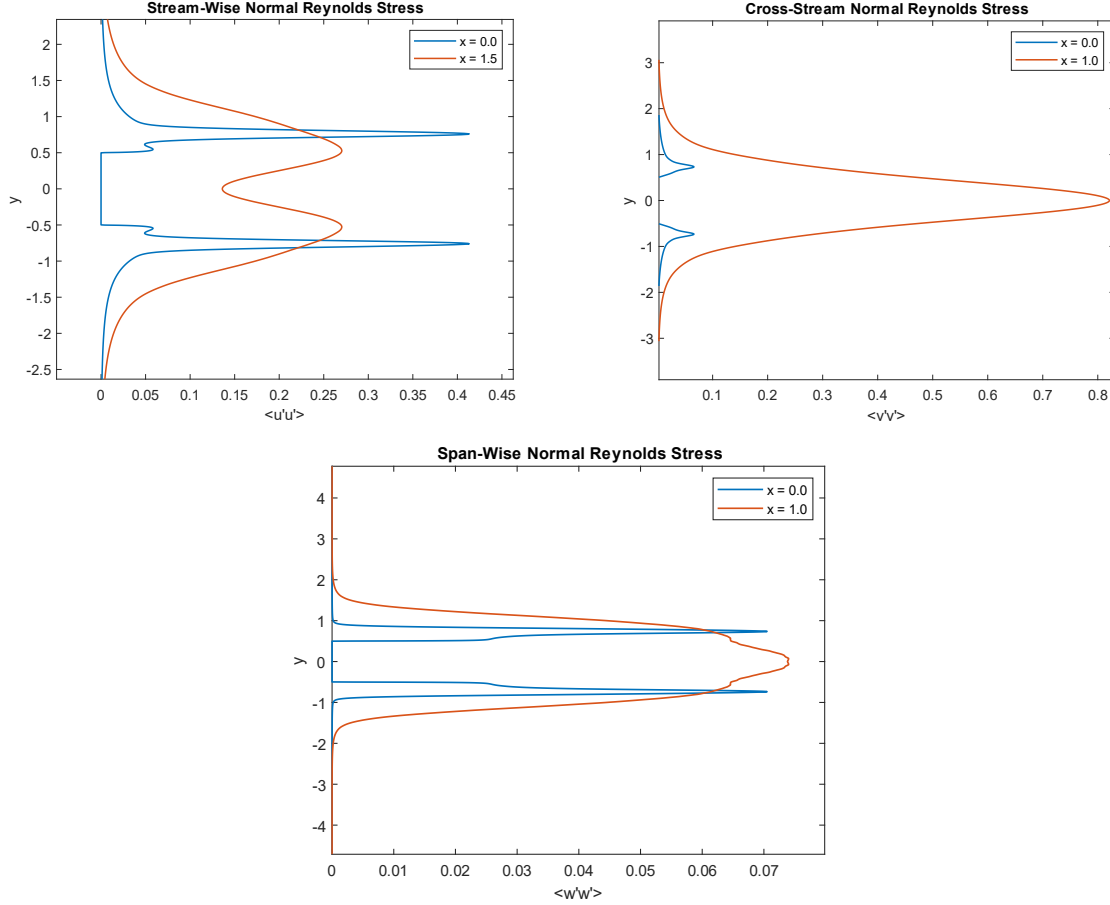


Figure 5. Normal Reynolds Stresses at $x = 0.0$ compared to $x = 1.0$ in: stream-wise direction (left), cross-stream direction (right), span-wise direction (bottom).

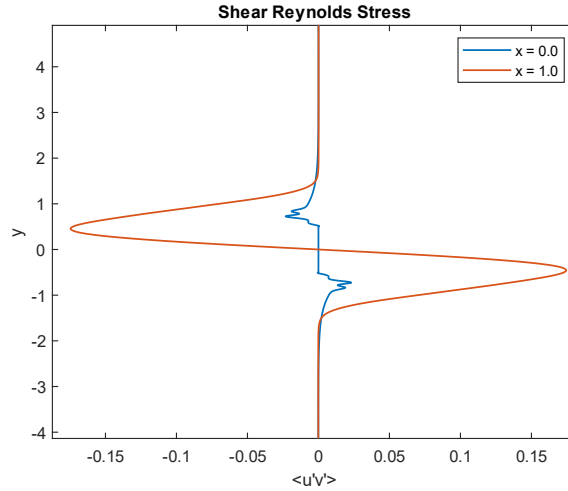


Figure 6. Reynolds Shear Stress at $x = 0.0$ compared to $x = 1.0$

3. Kolmogorov Length Scale

It is a common misconception that for having a DNS simulation, both the length and time steps of the simulation should be smaller than the Kolmogorov length and time scales. However, studies have shown that grid spacings equal to or smaller than η are considered too stringent because the Kolmogorov length scale is at the far end of the dissipative range. In this regard,

recent work has shown that most of the dissipation in a turbulent channel flow occurs at scales greater than 30η [1]. Kolmogorov length and time scales, defined as $\eta = (\nu^3/\langle \varepsilon \rangle)^{1/4}$ and $\tau_\eta = (\nu/\langle \varepsilon \rangle)^{1/2}$. Since the variables are time averaged, we will comment only on the former.

Figure 7 and Figure 8 show the ratio of the grid size in the x and y directions with respect to the Kolmogorov length scale, respectively (Δ_x/kol and Δ_y/kol). It can be seen that the maximum grid size to η ratio is in the order of 25 which indicated that most of the dissipation of the flow is captured, as discussed before.

There are two mechanisms of changes in these ratios: changes in the grid size by the tangent hyperbolic refinement function and changes in the mean dissipation rate of the flow $\langle \varepsilon \rangle$. These ratios increase with increasing grid size and decrease with increasing mean dissipation. Figure 7 left shows that for $-10 < x < -0.5$, the Δ_x/kol ratio decreases slowly as the grid is more and more refined, and there is minimal dissipation. In the region $0.5 < x < 20$, the ratio increases significantly due to two mechanisms: the grid size being increased as we move away from the obstacle and the most dominant one being the increased flow dissipation rate. The region where $-0.5 < x < 0.5$ is shown in Figure 7 right. Considering that the grid is finer near the corners of the square ($x=-0.5$ and $x=0.5$) and coarser when moving away from the corners, the graph shows a sudden drop in the ratio near $x=-0.5$ due to grid refinement, then grows steadily due to both grid stretching and increased dissipation rate. At $x=0.5$, the ratio drops again, however, to a higher value than at $x=-0.5$. Assuming a similar grid size at $x=0.5$ and $x=-0.5$, this shows that the dissipation rate at $x=0.5$ is higher than the one at $x=-0.5$.

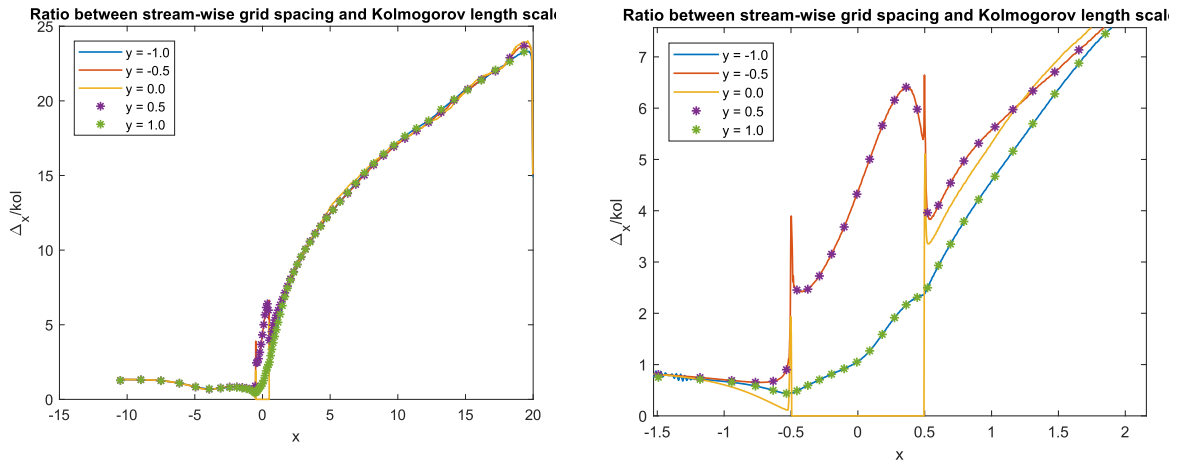


Figure 7. The ratio of the stream-wise grid spacing and Kolmogorov length scale.

Figure 8 shows the Δ_y/kol ratio. It can be seen that the high dissipation region is in the wake and SL of the obstacle and covers larger heights as x increases. Also, the dissipation seems to be higher at $x = 0.0$ compared to $x = 0.5$ and 1.5 .

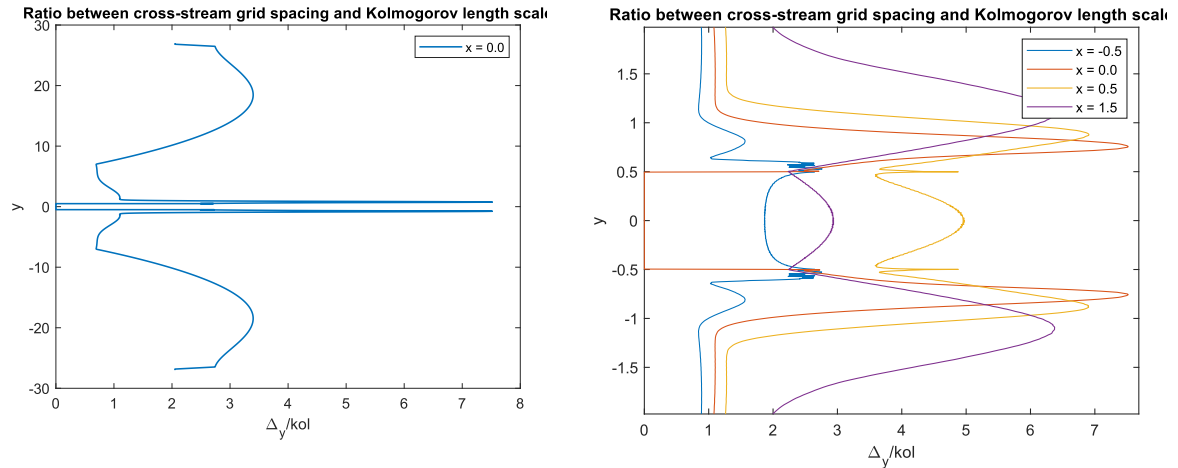


Figure 8. The ratio of the cross-stream grid spacing and Kolmogorov length scale.

4. Kinetic Energy and Turbulent Kinetic Energy

Despite the similarity in name, the Mean Kinetic Energy (MKE) and the Turbulent Kinetic Energy (TKE) show different flow attributes.

Figure 9 shows the MKE of the flow. Since the inlet MKE is 1, we see that most of the regions have this value. Upstream of the object, there's a stagnation area where the flow is slowed down to zero, and consequently, there will be a pressure build-up. Outside the BL and on the top and bottom faces of the square, we see the flow being accelerated and with the MKE of the flow up to 2 times the inlet. This is due to the object diverting the incoming air and pushing it to the sides, creating a smaller area for the inviscid flow above it, thus causing the velocity in that region to increase.

Inside the BL and in the wake region of the flow, we are observing lower MKE since the air is slowed down by the friction forces from the object. Even far away from the object, the flow has lower MKE in the wake due to the drag that it has created for the square (see momentum deficit in Aerodynamics)

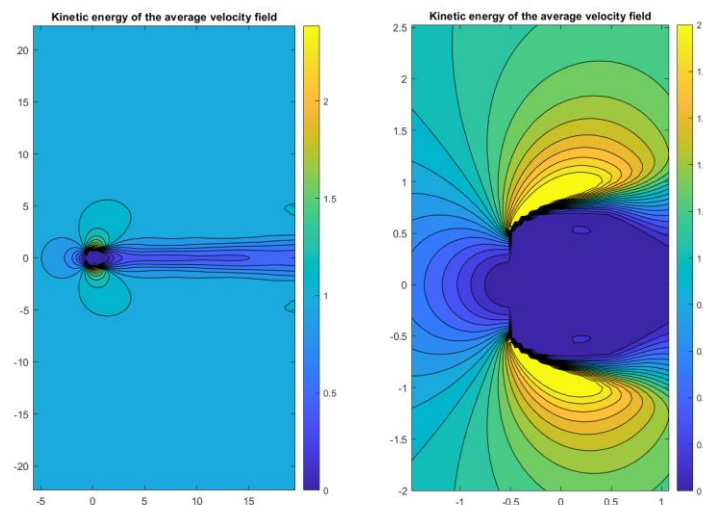


Figure 9. The kinetic energy of the average velocity field. Left: overall view. Right: body region.

Figure 10 shows the TKE of the flow. It can be seen that most of the areas of the domain are turbulent-free except for the wake, BL, and SL. It can be seen that immediately downstream of the body, there is an area of high TKE. This shows that a large eddy containing high energy is created at this location, and the TKE is reduced further downstream of the body as the turbulence dissipates.

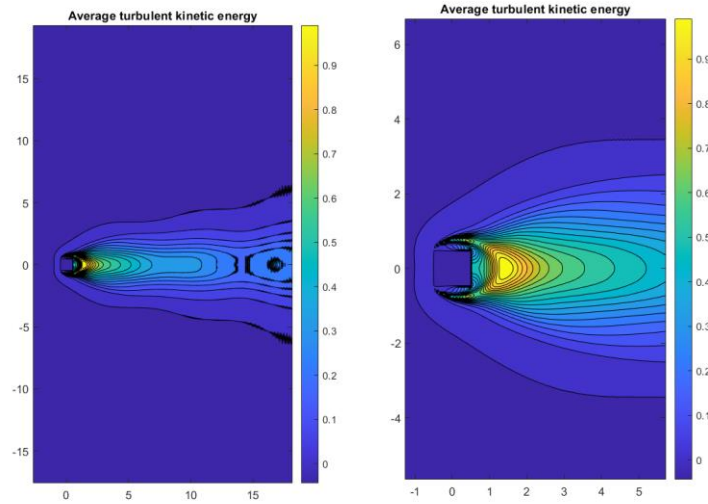


Figure 10. Turbulent kinetic energy of the average velocity field. Left: overall view. Right: body region.

5. Lift and Drag Dynamics

Figure 11 shows the time variation of the lift and drag coefficient for the first 300s. It can be seen that it takes almost 50 seconds for the flow to evolve for the von Karman vortex shedding process to start and to see oscillations in the lift coefficient. It can be seen that the drag coefficient averages around 2 with small variations, while the lift coefficient averages around zero but with significant variations. Since the D/Dt of vorticity in the domain should remain zero (Helmholtz's third theorem) each time that a counter-clockwise vortex is shed, the cylinder experiences positive lift, and each time that a clockwise vortex is shed, the cylinder experiences a negative lift.

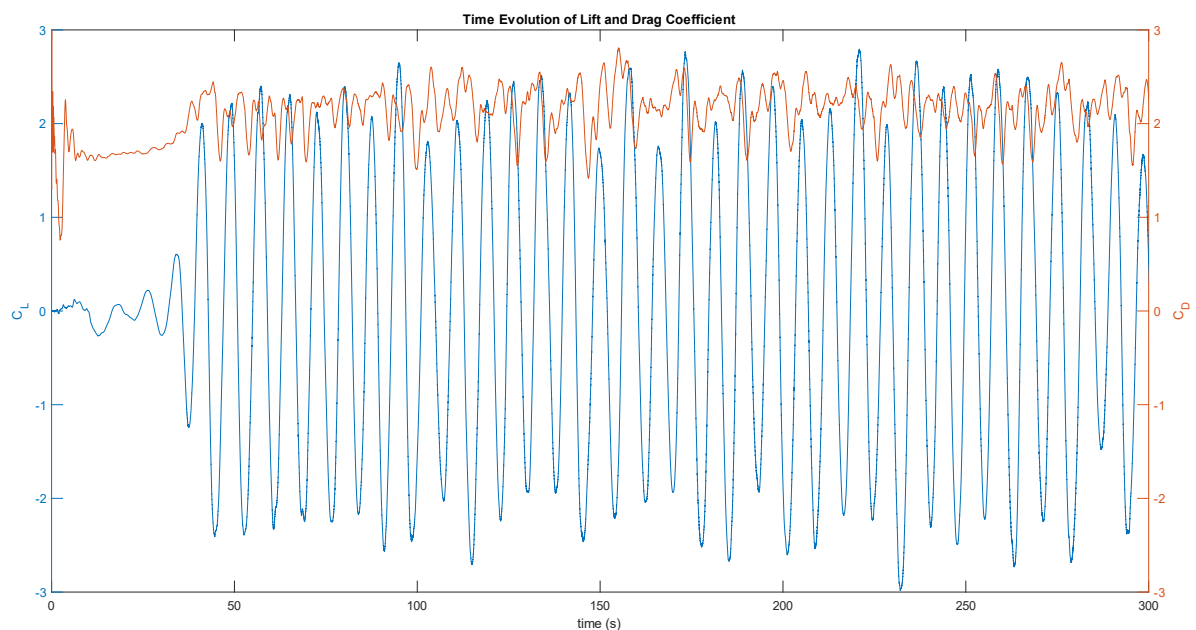


Figure 11. Time variation of the Lift and Drag Coefficient.

6. Conclusion

Based on the analysis of the flow characteristics around the obstacle, several key findings have been observed. The velocity profiles indicate a clear impact of the obstacle on the flow, with significant changes in velocity components and the presence of vortices. The Reynolds stresses and turbulent kinetic energy further illustrates the complex nature of the flow, highlighting the impact of the obstacle on turbulence and energy distribution.

The investigation into grid refinement and dissipation rate has provided valuable insights into the numerical aspects of the simulation, shedding light on the variations in flow behavior with different grid sizes and locations within the domain.

Furthermore, the examination of kinetic energy and its distribution has revealed the influence of the obstacle on flow acceleration, deceleration, and turbulence generation, particularly in the boundary layer and wake regions.

The analysis of lift and drag dynamics has demonstrated the periodic shedding of vortices and its impact on the lift and drag coefficients, aligning with theoretical expectations and providing a comprehensive understanding of the flow's aerodynamic characteristics.

In conclusion, the study has provided a detailed understanding of the flow behavior around the obstacle, encompassing velocity profiles, Reynolds stresses, grid refinement, kinetic energy, and lift and drag dynamics. These findings contribute to a deeper comprehension of the complex flow phenomena and can serve as a valuable reference for further research and practical applications in fluid dynamics and aerodynamics.

7. References

- [1] F. X. Trias, A. Gorobets, and A. Oliva, "Turbulent flow around a square cylinder at Reynolds number 22,000: A DNS study," *Computers & Fluids*, vol. 123, pp. 87–98, Dec. 2015, doi: 10.1016/j.compfluid.2015.09.013.
- [2] A. J. Smits, "Lectures in Fluid Mechanics Viscous Flows and Turbulence." Department of Mechanical Engineering Princeton University. [Online]. Available: <http://profs.sci.univr.it/~zuccher/downloads/FD-MAE553-Smits.pdf>
- [3] L. Davidson, "Fluid mechanics, turbulent flow and turbulence modeling", [Online]. Available: https://www.tfd.chalmers.se/~lada/postscript_files/solids-and-fluids_turbulent-flow_turbulence-modelling.pdf

8. Appendix I: MATLAB Code

```
clear all;

mypath1=[pwd,' \ Cyl22K\profiles']; %path of data files containing flow field
variables at different axial locations.

%%%%%%%%%%%%%%%%%%%%%%%%%%%%%%%%%%%%%%%%%%%%%%%%%%%%%%%%%%%%%%%%%%%%%%%%
% 1-Example of profile plots
%%%%%%%%%%%%%%%%%%%%%%%%%%%%%%%%%%%%%%%%%%%%%%%%%%%%%%%%%%%%%%%%%%%%%%%%

filename='Cyl22K_x150'; %file containing flow field variables.
A=readtable(fullfile(mypath1,filename), 'Delimiter', 'space', 'HeaderLines', 2,
'ReadVariableNames', false); %read the profiles data into the matrix A

%% plot for different xs

x=A.Var1;y=A.Var2;u=A.Var3;v=A.Var4;p=A.Var5;uu=A.Var6;vv=A.Var7;ww=A.Var8;uv=A.Va
r9;eps=A.Var10; % assign an intuitive variable to each column of the matrix A
Dx=0.5*(circshift(x,-1)-circshift(x,1));Dx(1)= Dx(2); Dx(end)= Dx(end-1); %size of
control volumes in x-direction % here the first and last elements of Dx or Dy may
be
% negative values. therefore we equate them to their neighboring cell's value.
% positive value of Dx and Dy.
% by using array shift function rather than for loops, we save
% computational expense.
Dy=0.5*(circshift(y,-1)-circshift(y,1));Dy(1)= Dy(2); Dy(end)= Dy(end-1); %size of
control volumes in y-direction
figure(1)
plot(u,y,'LineWidth',1.1)
ylabel('y');
xlabel('<u>')
title('Horizontal velocity profiles');
hold on
legend('x = 0.0' , 'x = 1.5' , 'x = 0.5' , 'x = -0.5')

figure(2)
plot(uu,y,'LineWidth',1.1)
ylabel('y');
xlabel('<u''u''>')
title('Stream-Wise Normal Reynolds Stress');
hold on
legend('x = 0.0' , 'x = 1.5' , 'x = 0.5' , 'x = -0.5')

figure(3)
plot(vv,y,'LineWidth',1.1)
ylabel('y');
xlabel('<v''v''>')
title('Cross-Stream Normal Reynolds Stress');
hold on
legend('x = 0.0' , 'x = 1.0' , 'x = 0.5' , 'x = -0.5')

figure(4)
plot(ww,y,'LineWidth',1.1)
ylabel('y');
xlabel('<w''w''>')
title('Span-Wise Normal Reynolds Stress');
```

```

hold on
legend('x = 0.0' , 'x = 1.0' , 'x = 0.5' , 'x = -0.5')

figure(5)
plot(uv,y,'LineWidth',1.1)
ylabel('y');
xlabel('<u''v''>');
title('Shear Reynolds Stress');
hold on
legend('x = 0.0' , 'x = 1.0' , 'x = 0.5' , 'x = -0.5')

nu=1/22000; %kinematic viscosity L=1 U=1 Re=UL/nu=22000

% plot the ratio of the CROSS-STREAM grid spacing to the Kol scale
figure(6)
Kol=(nu^3./abs(nu*eps)).^0.25; %Kolmogorov length scale
plot(Dy./Kol,y,'LineWidth',1.1)
ylabel('y');
xlabel('\Delta_y/kol');
title('Ratio between cross-stream grid spacing and Kolmogorov length scale');
hold on
legend('x = 0.0' , 'x = 1.0' , 'x = 0.5' , 'x = -0.5')

%% plot for different ys

x=A.Var1;y=A.Var2;u=A.Var3;v=A.Var4;p=A.Var5;uu=A.Var6;vv=A.Var7;ww=A.Var8;uv=A.Var9;eps=A.Var10; % assign an intuitive variable to each column of the matrix A
Dx=0.5*(circshift(x,-1)-circshift(x,1));Dx(1)= Dx(2); Dx(end)= Dx(end-1); %size of control volumes in x-direction % here the first and last elements of Dx or Dy may be
% negative values. therefore we equate them to their neighboring cell's value.
% positive value of Dx and Dy.
% by using array shift function rather than for loops, we save
% computational expense.
Dy=0.5*(circshift(y,-1)-circshift(y,1));Dy(1)= Dy(2); Dy(end)= Dy(end-1); %size of control volumes in y-direction
% here the first and last elements of Dx or Dy may be
% negative values. therefore we set any negative value to the smallest
% positive value of Dx and Dy.
% by using array shift function rather than for loops, we save
% computational expense.

figure(1)
plot(x,v,'LineWidth',1.1)
xlabel('x');
ylabel('<v>');
title('Vertical Velocity Profiles');
hold on
legend('y = -1.0','y = -0.5', 'y = 0.0' , 'y = 0.5','y = 1.0')

nu=1/22000; %kinematic viscosity L=1 U=1 Re=UL/nu=22000

% plot the ratio of the STEAM-WISE grid spacing to the Kol scale
figure(2)
Kol=(nu^3./abs(nu*eps)).^0.25; %Kolmogorov length scale
plot(x,Dx./Kol,'LineWidth',1.1)
xlabel('x');
ylabel('\Delta_x/kol')

```

```

title('Ratio between stream-wise grid spacing and Kolmogorov length scale');
hold on
legend('y = -1.0', 'y = -0.5', 'y = 0.0' , 'y = 0.5', 'y = 1.0')

```

```

%% Contour plots

```

```

mypath2='D:\College\References 98\1.EMJMD\1. 2023-2024 01\Turbulence
Modeling\My\Assignment 2\Cyl22K\XYsection'; %your path of data files

```

```

%%%%%%%%%%%%%%%%%%%%%%%%%%%%%%%%%%%%%%%%%%%%%%%%%%%%%%%%%%%%%%%%%%%%%%%%
% 2-Example of 2D average field plot
%%%%%%%%%%%%%%%%%%%%%%%%%%%%%%%%%%%%%%%%%%%%%%%%%%%%%%%%%%%%%%%%%%%%%%%%

```

```

filename='Cyl22K_XY.dat';
B=readtable(fullfile(mypath2,filename), 'Delimiter', 'space', 'HeaderLines', 3,
'ReadVariableNames', false);
x=B.Var1;y=B.Var2;u=B.Var3;v=B.Var4;w=B.Var5;p=B.Var6;uu=B.Var7;vv=B.Var8;ww=B.Var
9;uv=B.Var10;eps=B.Var11;
XY=[(1:size(x))',x,y]; XYsortbyX=sortrows(XY,2); XYsortbyY=sortrows(XY,3);
%Size of control volumes in x-direction:
Dx=0.5*(circshift(XYsortbyY(:,2),-1)-
circshift(XYsortbyY(:,2),1));Dx(Dx<0)=min(abs(Dx));
auxDx=sortrows([XYsortbyY(:,1),XYsortbyY(:,2),Dx],1);Dx=auxDx(:,3);
%Size of control volumes in y-direction:
Dy=0.5*(circshift(XYsortbyX(:,3),-1)-
circshift(XYsortbyX(:,3),1));Dy(Dy<0)=min(abs(Dy));
auxDy=sortrows([XYsortbyX(:,1),XYsortbyX(:,2),Dy],1);Dy=auxDy(:,3);

```

```

% creating meshgrid
res=1000; %linspace resolution
numlevel=20; %number of contour levels
xv=linspace(min(x),max(x),res);
yv=linspace(min(y),max(y),res);
[X,Y] = meshgrid(xv,yv);

```

```

figure(3)
quiver(x,y,u,v);
axis equal;
title('Average velocity field');

```

```

figure(4)
VOL = griddata(x,y,Dx.*Dy,X,Y);
contourf(X,Y,VOL,numlevel);
axis equal
title('Volumes');
contourcbar

```

```

figure(5)
K = griddata(x,y,u.^2+v.^2,X,Y); % here, <w> is neglected since w averages around
0 in this setup of simulation
contourf(X,Y,K,numlevel);
axis equal
title('Kinetic energy of the average velocity field');
contourcbar

```

```

figure(6)
Kt = griddata(x,y,uu+vv+ww,X,Y);

```



```

contourf(X,Y,Kt,numlevel);
axis equal
title('Average turbulent kinetic energy');
contourcbar

```

```

%% Lift and Drag

```

```

mypath2='D:\College\References 98\1.EMJMD\1. 2023-2024 01\Turbulence
Modeling\My\Assignment 2\Cyl22K\dynamics'; %your path of data files

```

```

%%%%%%%%%%%%%%%%%%%%%%%%%%%%%%%%%%%%%%%%
% 2-Example of 2D average field plot
%%%%%%%%%%%%%%%%%%%%%%%%%%%%%%%%%%%%%%%%

```

```

filename='Cyl22K_drag_and_lift';
B=readtable(fullfile(mypath2,filename), 'Delimiter', 'space', 'HeaderLines', 2,
'ReadVariableNames', false);
t=B.Var2;D=B.Var4;L=B.Var5;
figure(7)
title('Time Evolution of Lift and Drag Coefficient')
yyaxis left
plot(t,L)
ylabel('C_L')
xlabel('time (s)')

yyaxis right
plot(t,D)
ylabel('C_D')

```